

Torque Performance of Permanent Magnet Synchronous Motor based on Different Rotor Structures

Firdaus Talip¹, Roziah Aziz^{1*}

¹Faculty of Electrical and Electronic Engineering,
Universiti Tun Hussein Onn Malaysia, Batu Pahat, Johor, 86400, MALAYSIA

*Corresponding Author Designation

DOI: <https://doi.org/10.30880/eeee.2023.04.02.093>

Received 03 July 2023; Accepted 29 August 2023; Available online 30 October 2023

Abstract: Permanent magnet synchronous motor (PMSM) consists of permanent magnet at the rotor to produce a constant magnetic field. Permanent magnet synchronous motor classified into two categories which is Interior Permanent Magnet Synchronous Motor (IPMSM) and Surface Permanent Magnet Synchronous Motor (SPMSM). For IPMSM, a permanent magnet is embedded inside the rotor core while for SPMSM, the permanent magnet is attached at the surface of the rotor. IPMSM offers high torque and power density. However, it produces high cogging torque compared to SPMSM. The performances of IPMSM are also related to the permanent magnet materials that are used to produce constant magnetic flux for the motor. In this paper, the design study of 4 pole 24 slots with different rotor structure parameters is studied to compare the torque performances with the same type of permanent magnet materials. The permanent magnet materials that have been selected are Neodymium Iron Boron (NdFeB). Initially, design procedures of IPMSM including parts drawing, material and condition setting, the properties setting are all explained. Then, a coil arrangement test is conducted to perform 3 phase armature coil arrangement. Finally, the purpose of this paper is to find out which rotor structure can produce higher performance.

Keywords: Permanent Magnet Synchronous Motor, Torque Performances, Interior Permanent Magnet, Rotor Structure, Permanent Magnet.

1. Introduction

A permanent magnet synchronous motor is a motor that uses a permanent magnet in a rotor. A permanent magnet synchronous motor (PMSM) produces high torque density, very efficient and it can operate for a long time [1]. The most common type is Surface Permanent Magnet (SPM) machines and Interior Permanent Magnet (IPM) machines. The difference between IPM and SPM is their topology. As for SPM, the permanent magnet has been placed at the outside of the rotor core. For IPM, the permanent magnet embedded inside the rotor core. Among the differences for their topology for PMSM, IPM are less demagnetized than SPM [2]. Over the past year, all producers have chosen the Interior

*Corresponding author: roziah@uthm.edu.my

2023 UTHM Publisher. All rights reserved.

publisher.uthm.edu.my/periodicals/index.php/eeee

Permanent Magnet Synchronous Machine (IPMSM) as the best option in automotive. IPMSM has been widely applied to the electric vehicle field and aerospace industry from all over the world [3]. The reason behind it, because it does very good in performance of high-power density, high efficiency, and high reliability.

The interior permanent magnet motor has benefits over the surface permanent magnet motor, including strong overload capacity, high mechanical strength, quick dynamic reaction, and a wide range of weak magnetic speed regulation. There are three types of internal rotor construction: radial, tangential, and mixed. The output torque ripple of the V structure is reduced when compared to the other rotor structure. Many professionals are presently investigating how to alter certain factors to enhance motor function. It is more important to increase motor performance from the motor's construction than it is to reduce slot torque in control [4]. As you know the most important thing in torque performance is permanent magnet. The torque performance has also been affected by the rotor structure and characteristics. The effect of demagnetized will greatly reduce the performance of IPM [3]. This paper investigates the different rotor structures that affected the torque performance analysis. The design that been chosen for this work is 24 slot and 4 poles with the U-rotor and C-rotor structure.

The chosen of 24 slot and 4 poles because the motor configuration offers a balance between efficiency and performance, distributing winding coils efficiently, reducing losses like cogging and eddy currents. This design reduces torque ripples, improves performance, and reduces noise and vibration levels. It also aligns well with manufacturing capabilities and efficiency, potentially reducing production costs and complexity. U-rotors have been chosen because they offer higher torque density, better cooling characteristics, and lower cogging torque, making them suitable for high-power applications with high power density. Their open design enhances airflow and heat dissipation, making them ideal for thermal management. Additionally, U-rotors are easier to manufacture, potentially reducing costs and simplifying the production process. Lastly, for the C-rotor is because the C-rotor structure minimizes cogging torque by using a skewed or slotted rotor design, reducing interaction between rotor and stator teeth. This improves motor operation smoothness and control at low speeds. C-rotor structures also exhibit improved flux-weakening capability, allowing motors to maintain torque output beyond nominal speed range. This design reduces rotor losses, such as eddy current and hysteresis losses, resulting in improved motor efficiency [4].

For torque performance, permanent magnets have become an important role after the rotor parameters. Due to the complex structure of rotor, the torque performance of the motor greatly affected by the structural parameters of the rotor [5]. There are many types of rotor structure such as flux barrier shape, number of layers, rib width, air gap length and permanent magnet parameters such as permanent magnet width and thickness on torque performance. For this work, an observation must be made on the value of torque performance analysis based on different rotor structures and different permanent magnet parameters. Due to their high torque density and excellent efficiency, IPMSM with V-shaped permanent magnet rotors are frequently employed as traction motors in electric vehicles [4]. Despite the merits of the IPMSM with V-shape rotor, issues still exist, setting up the scope for further research investigations. It has the disadvantages of inevitable torque ripple due to the non-sinusoidal air-gap flux density and the utilization of the reluctance torque. As the torque ripple affects the vibration and noise it should be reduced.

The choice of using a magnet dimension has a significant impact on performance. Optimization is applied to achieve the required torque characteristics by varying the permanent magnet size with fixed volume and length. Many results showed that the motor torque was higher with a wider magnet scale and fewer magnets per pole. Additionally, the use of thicker magnets has improved motor efficiency. Therefore, this must be considered when designing a motor according to torque specifications [6].

2. Materials and Methods

The design requirement for this interior permanent magnet U and C type is 24 slot and 4 poles with the armature coil current is 5A. Figure 1 shows a block diagram of the process to design the motor. Each part of motor namely stator, rotor, armature coil and permanent magnet and this will design by using Geometry Editor. Figure 2 shows the block diagram of the JMAG Designer process. JMAG Designer used to set the materials, circuit, condition and doing mesh analysis until get the result.

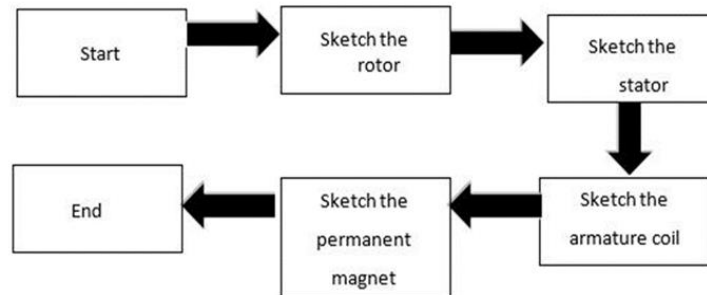


Figure 1: Block diagram the process to design the motor

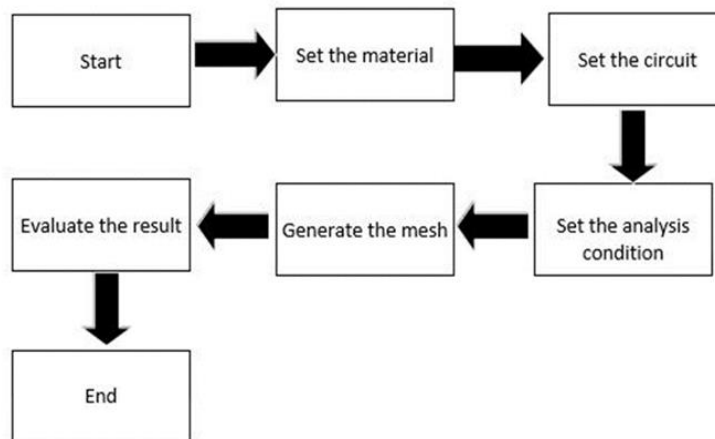


Figure 2: Block diagram of the JMAG Designer process

After all the parts of the motor have been constructed, the full design will appear by import model to the JMAG Designer. Figure 3(a) shows the completed design of U- rotor structure model while Figure 3(b) illustrates the completed design of C-rotor structure model.

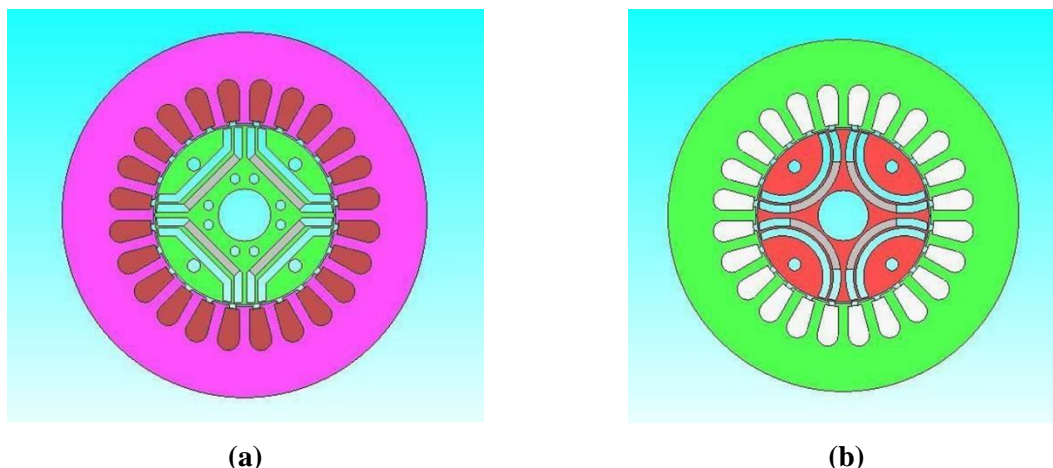


Figure 3: Completed Design of (a) U-rotor and (b) C-rotor structure model

This work implements the usage of JMAG Designer software that is used to simulate the motor structure design. The workflow for this work is shown in Figure 4.

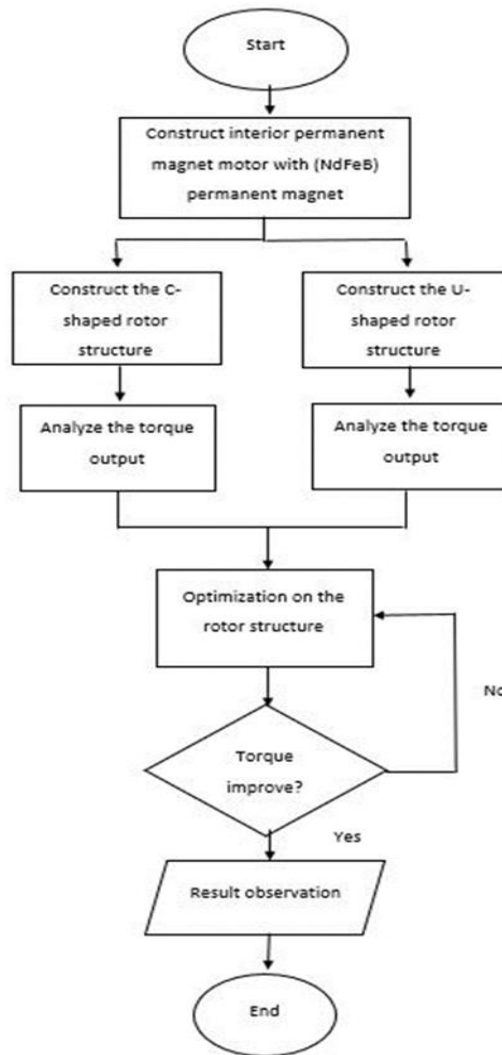


Figure 4: Flowchart for the whole process

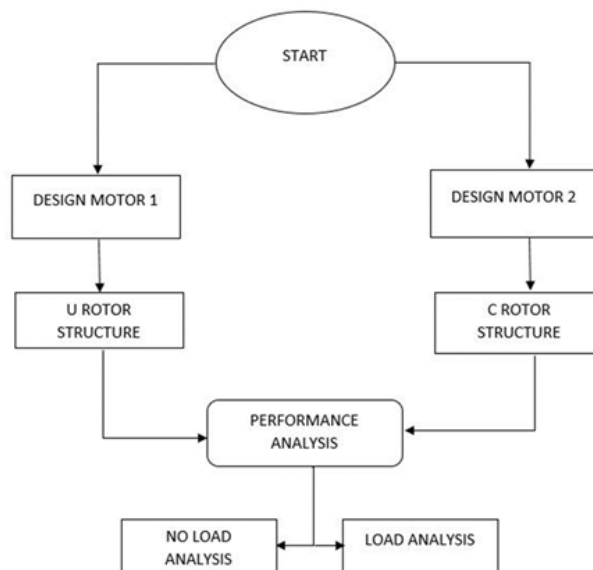


Figure 5: Different rotor selection workflow

After the material, condition, and circuit connection of the FEM coil have been determined, the JMAG Analysis tool is used to conduct magnetic research on the motor. Open a new magnetic case study for the design that has already been developed to run JMAG analysis for magnetic studies. Active Case Study was run to obtain the output data corresponding to the design specification of the motor. Once the case solver is finished, the following results are available to be obtained which are torque, magnetic flux density, iron losses, copper losses, efficiency, and a graph of hysteresis losses. JMAG analysis uses both No Load Test and Load Test to evaluate the motor's performance. Mesh must be generated to carry out both tests. The mesh can be made with a 1mm mesh size. Figures 5 and 6 show the flowchart to conduct the test analysis.

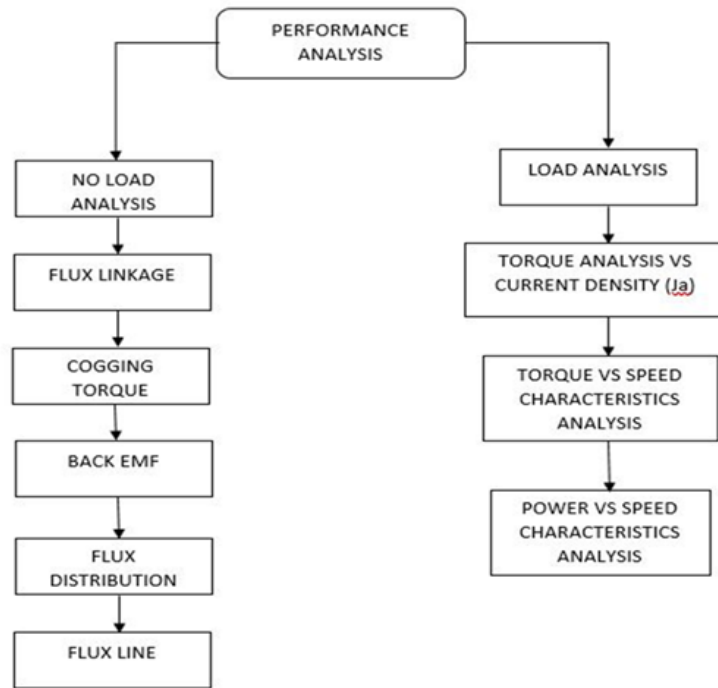


Figure 6: Performance analysis workflow

3. Results and Discussion

The complete design of the motor is shown for this section. There are four main parts that need to be known for the completed design of motor which are stator, rotor, armature coil and permanent magnet. For this work, two designs of motor have been proposed with two different rotor structures which are U-rotor structure and C-rotor structure.

3.1 24 Coil Flux Linkage Test

Before going to the next result, this study must conduct the 24-coil flux linkage test first. The result come out from the circuit that have done by refer to the 24 slots of armature coil and 4 poles motor as shown in Figure 7. The graph that has been obtained then transferred to Microsoft Excel. From the result obtained, a conclusion can be made that some coils have the same pattern as an example C1, C6, C8, C13, C18, C20, C23 and C11. For the pattern is C2, C4, C7, C9, C14, C16, C19 and C21. For the last pattern is C3, C5, C10, C12, C15, C17, C22 and C24.

3.2 3 Coil Flux Linkage Test

To make the 24-coil become 3 coils. The three same pattern that been stated above must be combined to make 8 coils per phase. As a result of the combination, will form three types of waveforms and produce three flux patterns. Figure 8 shows the result of 3 coil flux linkage test.

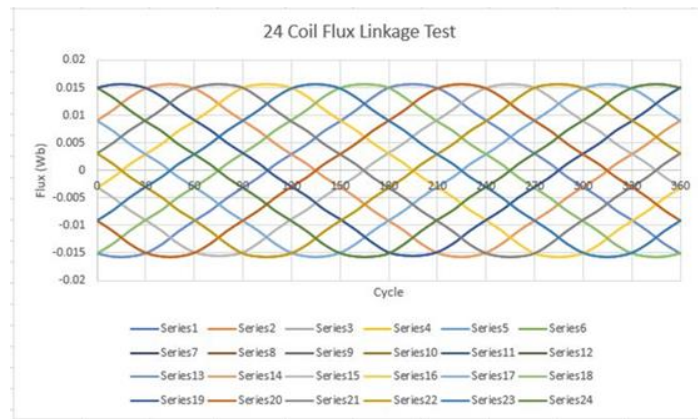


Figure 7: 24 coil flux linkage tests

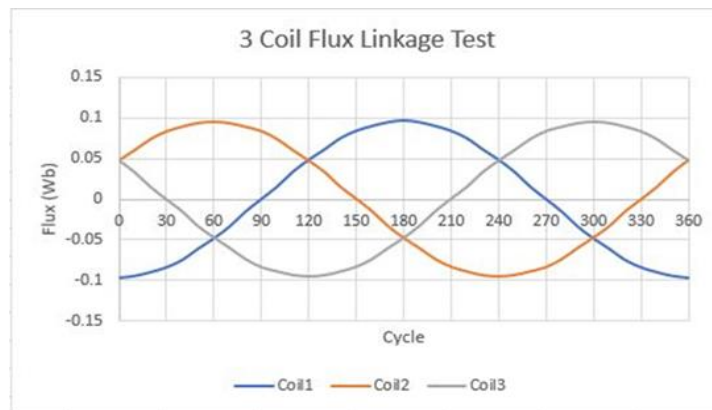


Figure 8: 3 coil flux linkage tests

3.3 Flux Distribution

This test is for the analysis of flux distribution inside the suggested motors as it has been divided into various colours to determine their frequency. As a result, the purple colour represents the lowest flux while the red colour represents the maximum flux. The research that follows discusses the flux density distribution that is depicted in Figure 9.

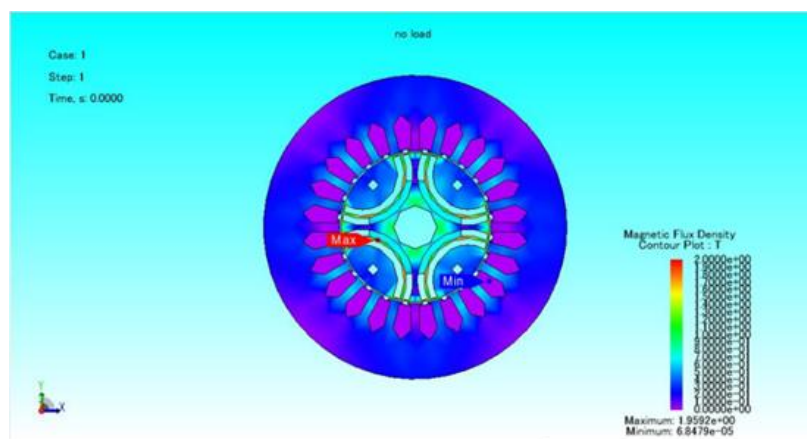


Figure 9: Result for flux distribution

3.4 Flux Line

Under open circuit conditions, flux orientation investigations were carried out in which all machine topologies are compared at zero-degree rotor position. To determine whether the flux produced by the permanent magnet and armature coil deviates from its magnetization pattern, flux line figures are utilized. Strayed flux will result in a larger back-EMF and negatively impact the motor's design. The

flux line for a motor design with a different rotor structure, such as a U-rotor or C-rotor, is shown in Figure 10. The flux traces, however, fight against one another since they want to stretch as far as they can from different flow traces. The exchange location of the stator has made it possible for flux to move from one rotor structure to the next, increasing the efficiency of this effect's magnetizing attraction. Due to its lengthy travel time and consequently worse overall flux linkage quality, the flux will fail.

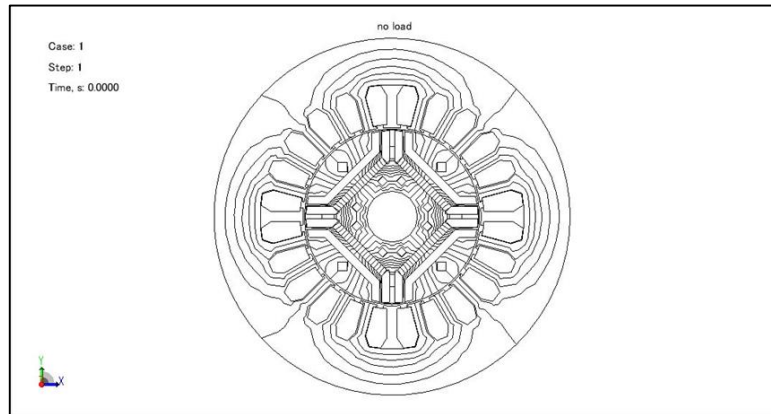


Figure 10: Result for flux line

3.5 Cogging torque

Cogging torque, which can cause noise, speed ripples, vibration, resonances, and even damage to the motor's construction, is essentially the result of the interaction between the rotor PM and stator slots. The cogging torque of each of the two versions of the suggested IPMSM motors is shown in Figure 11. According to the graph, the cogging torque for the U-rotor IPMSM has a peak-to-peak measurement of 0.0635 Nm, whereas the cogging torque for the C-rotor IPMSM has a peak measurement of 0.1324 Nm. The number of torque should not be greater than the average torque by more than 10% because this results in significant vibration.

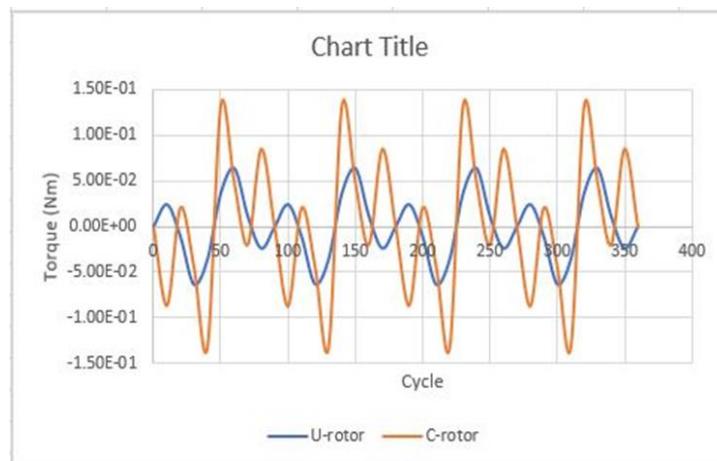


Figure 11: Result for cogging torque

3.6 Back EMF

The back electromotive force is produced by the relative motion of the magnetic field and coil. When the coil rotates inside the magnetic field, it is induced. At a certain value, the back EMF is claimed to control the motor's speed and to be equal to or lower than the applied voltage, in this example 415V. This guarantees that the motor operates safely and without harming the coils. Figure 12 displays the back-emf graphs for the two models at a speed of 1200 rpm for the motors. In the graph below show the value of the fundamental (F) and harmonics (H). The fundamental component of the back EMF is the electrical frequency proportional to rotor speed and determines the motor's speed-torque

relationship. Harmonics, integer multiples of the fundamental frequency, are additional frequency components resulting from non-linear factors like magnetic saturation, stator winding distribution, and rotor slotting. They introduce distortions and affect performance, such as torque ripples, efficiency, and noise. Incorporating harmonics in back EMF waveform analysis is crucial for accurate representation and minimizing undesirable effects like torque ripple or excessive losses.

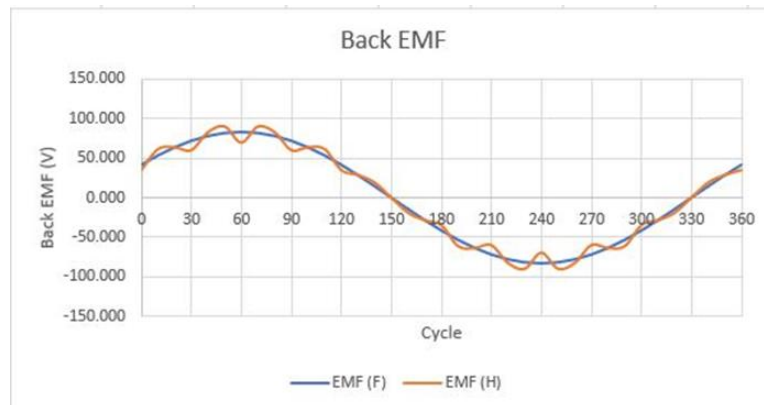


Figure 12: Result for back EMF

3.7 Torque vs Various Armature Coil Current Density, J_a

When a varied current value is injected into the motor FEM coil, the torque of various J_a will be analysed to verify the torque variable pattern. Torque is measured at different J_a for two model motors with variously constructed structures. During the load study, the J_a value of the armature current density is determined, ranging from 0 to 30 Arms/mm². Figure 13 illustrates the J_a vs torque graph. Torque vs various J_a graphs show that the torque is increased when the injected current density, J_a is increased. However, the maximum torque or torque at maximum A for different rotor structures is not same. Greatest torque was produced at $J_a = 30$ A/mm, when using a U-rotor structure model compared to C-rotor structure model

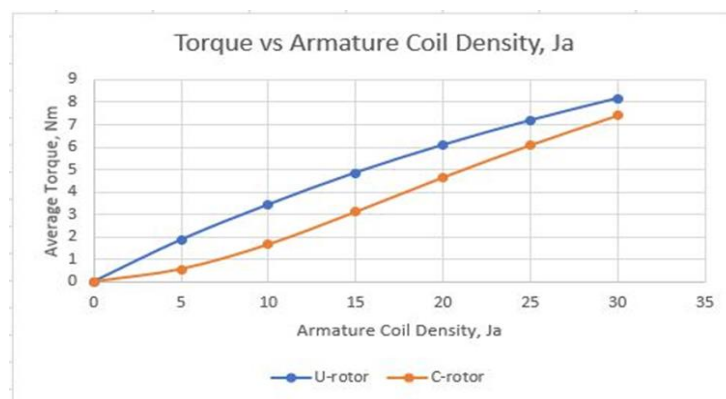


Figure 13: Result for torque vs J_a

3.8 Torque and Power vs Speed Characteristics

Based on the graph and result obtained for the U-rotor and C-rotor, the differences between these two parameters are because the choice of rotor structure does not necessarily determine the motor's power, speed, or torque characteristics. The result obtained from the graph U-rotor shown in Figure 14 presents that at the speed of 741.175 rpm it begins to decrease when operated beyond the base speed region due to high iron loss. The maximum output power is 6.331 kw before decreasing to 3.552 kw at the speed 988.995 and increase until 4.84 kw at maximum speed.

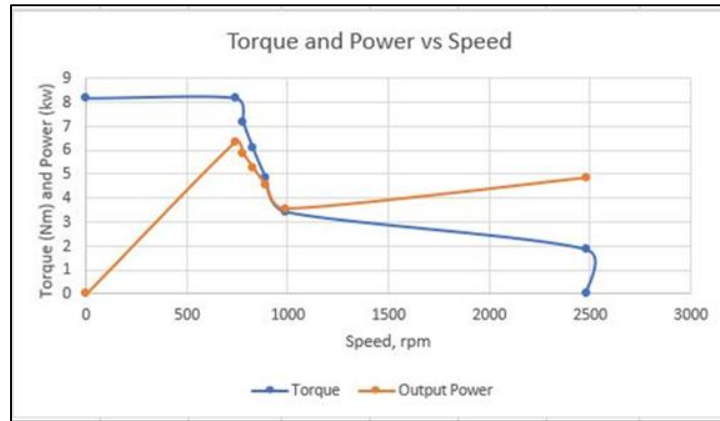


Figure 14: Result for torque and power vs speed U-rotor

While from the graph C-rotor shown in Figure 15, it can be concluded that the value achieved a highest output torque 7.401 Nm at base speed of 1161.79 and begins to decrease when the speed is increase. Furthermore, the maximum output power got from this motor is 9 kw at base speed and decreases until the speed is 3760.32. Unfortunately, the power decreased again at maximum speed 5362.12 and produced 3.13 kw.

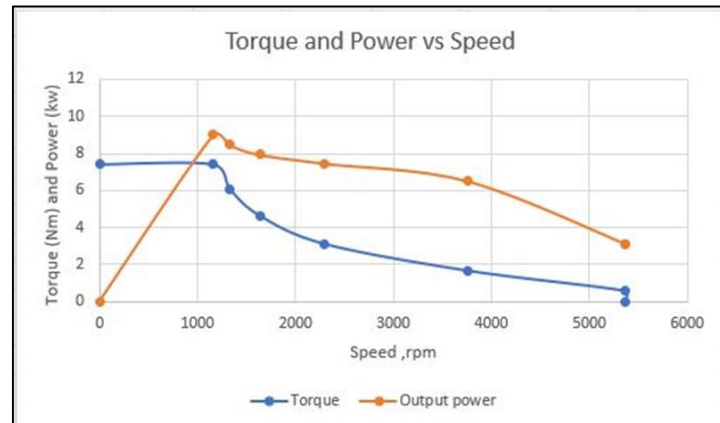


Figure 15: Result for torque and power vs speed C-rotor

The value that gained is influenced by many factors as an example the number of elements, such as the design specifications, materials, winding configuration, and control techniques used for designing this motor really give big impacted on the value of torque and power vs speed. A motor's output of torque, speed and power is determined by its overall design and optimization process, which considers variables including the number of poles, stator and rotor diameters, magnetic materials, and control algorithms. An all-encompassing design strategy is needed to optimize a motor's performance, including the appropriate balance of torque, speed, and power. This calls for careful study, simulation, testing and consideration of numerous design factors and performance criteria.

4. Conclusion

In this paper, two design motors with different rotor structure parameters U-rotor structure and C-rotor structure have been studied. Neodymium-Iron Boron (NdFeB) is the material used for this experiment. The steps involved in designing an IPMSM. To verify each armature coil phase and to demonstrate how the machine works, the coil arrangement test for each design motor has been evaluated. With different rotor structures, tests on the two motors' capabilities, including cogging torque, starting torque, maximum speed, power, and armature coil current density, have been done. The proposed model has each distinctive performance. For this work, the selected motor for this investigation based on the performances of its motor in the scope of torque and power of the motor.

Motor with U-rotor produced higher torque compared to C-rotor. However, the maximum power produced by motor with U-rotor slightly lower than motor with C-rotor. Lastly, the speed for the two motors also have been compared as a result motor with C-rotor produce more speed than the U-rotor.

In conclusion, both motors have their own advantages, and they can be used in different work concepts. For example, a motor that uses a U-rotor can be used for work that requires high torque but uses low power and speed, while for the motor that uses C-rotor it can be used for work that uses power and high speed compared to torque. Overall, two different motors, which is U-rotor and C-rotor are allowed to tolerate some severe working condition.

Acknowledgement

The authors would like to thank the Faculty of Electrical and Electronics Engineering, Universiti Tun Hussein Onn Malaysia for its support.

References

- [1] Deaconu, A. S., Ghița, C., Năvrănescu, V., Chirilă, A. I., Deaconu, I. D., & Staton, D. (2012). Permanent magnet synchronous motor thermal analysis.
- [2] Wang, A., Jia, Y., & Soong, W. L. (2011). Comparison of five topologies for an interior permanent-magnet machine for a hybrid electric vehicle. *IEEE transactions on Magnetics*, 47(10), 3606-3609.
- [3] Ali, S. N., Hanif, A., & Ahmed, Q. (2016, January). Review in thermal effects on the performance of electric motors. In *2016 International Conference on Intelligent Systems Engineering (ICISE)* (pp. 83-88). IEEE.
- [4] Gao, P., Sun, X., Gerada, D., Gerada, C., & Wang, X. (2020). Improved V-shaped interior permanent magnet rotor topology with inward-extended bridges for reduced torque ripple. *IET Electric Power Applications*, 14(12), 2404-2411.
- [5] Liang, J., Liu, G., Wang, H., & Liu, H. (2018, December). Torque Performance Analysis of Permanent Magnet Assisted Synchronous Reluctance Motor Based on Rotor Structure Parameters. In *2018 IEEE Student Conference on Electric Machines and Systems* (pp. 1-5). IEEE.
- [6] Yulianto, K., Yusivar, F., & Sudiarto, B. (2021, June). The Influence of Magnet Number and Dimension on Torque Characteristics in the Interior Permanent Magnet Synchronous Motor (PMSM). In *IOP Conference Series: Materials Science and Engineering* (Vol. 1158, No. 1, p. 012006). IOP Publishing.